

Molybdenum diboride nanoparticles as highly efficient electrocatalyst for the hydrogen evolution reaction

Supporting Information

Palani R. Jothi,^{[a] [c]#} Yuemei Zhang,^{[a] [c]#} Jan P. Scheifers,^[a] Hyounmyung Park,^{[a] [b] [c]} Boniface P.T. Fokwa^{*[a] [b] [c]}

-
- [a] Department of Chemistry
University of California, Riverside
Riverside, CA 92521, USA
E-mail: bfokwa@ucr.edu; WWW: fokwalab.ucr.edu
- [b] Department of Chemical and Environmental Engineering
University of California, Riverside
Riverside, CA 92521, USA
- [c] Center for Catalysis,
University of California, Riverside
Riverside, CA 92521, USA
- # P.R.J. and Y.Z. contributed equally.

Table of contents

- I. Synthesis of *nano*-MoB₂**
- II. Computational details**
- III. Characterizations**
- IV. Tables**
- V. Figures**
- VI. References**

I. Synthesis of *nano-MoB₂*

All the chemicals were of analytical grade and used without any further purification. In a typical synthesis, 1 mmol of anhydrous MoCl₅ (99.9% purity) was mixed finely with 2.5 mmol of MgB₂ (99.9% purity) in a glove box and pressed into pellets. The pellets were transferred to a quartz tube which was then evacuated and sealed in Ar atmosphere. The quartz tube was placed in a programmable furnace and heated to 650 °C for 24 hours, then cooled to room temperature with the same heating and cooling rate (2 °C/minute). To remove MgCl₂, the product was dispensed into con. HCl (10%). The resulting boride product was washed in succession with deionized water and ethanol for several times. Finally, the product was dried at 120 °C for overnight in an oven.

II. Computational details

DFT calculations were applied to evaluate the H-surface binding energy ΔE_H on Pt {111}, Mo {110}, Mo- and B- terminated MoB₂ {001}, mixed Mo/B MoB₂ {110} and MoB₂ {101}, Mo- and B- terminated MoB₂ {100} surfaces. Total energy calculations were performed using the projector augmented wave (PAW) method of Blöchl^{1, 2} coded in the Vienna ab initio simulation package (VASP).³ All VASP calculations employed the generalized gradient approximation (GGA) with exchange and correlation treated by the Perdew-Burke-Enzerhoff (PBE) and revised PBE (revPBE) functionals, respectively, for structure relaxation and single energy calculations.^{4, 5} The convergence threshold for structural relaxation was set to be 0.02 eV/Å in force. The cutoff energy for the plane wave calculations was set to 500 eV and the Brillouin zone integrations were carried out using a 11 × 11 × 3, 13 × 9 × 3, 9 × 9 × 3, 3 × 7 × 11, 11 × 7 × 3 and 3 × 3 × 11 k-point mesh for Pt {111}, Mo {110}, MoB₂ {001}, MoB₂ {110}, MoB₂ {101} and MoB₂ {100} surfaces, respectively. The surfaces were constructed by cleaving the bulk Pt, Mo and MoB₂ structures into two dimensional (2D) slabs by choosing the right surface and enough vacuum (more than 13 Å) between slabs to avoid inter-slab interactions. The resulting Pt slab contains three metal layers, the Mo slab incorporates four metal layers, the Mo-terminated MoB₂ {001} slab has four Mo layers and three B layers, the B-terminated MoB₂ {001}, as well as the B- and Mo-terminated MoB₂ {100} slabs contain four Mo layers and

four B layers, and finally the MoB₂ {101} and {110} slabs hold four and six [MoB₂] layers, respectively. The so obtained new 2D cell contains four metal atoms in each metal layer for all four cases, while for MoB₂ {001} and {100} surfaces each boron layer contains eight boron atoms and each layer of the MoB₂ {110} and {101} mixed surface has eight boron and four molybdenum atoms. The hydrogen coverage on each surface was calculated by dividing the number of H atoms adsorbed on the surface by the number of metal atoms (or half the number of B atoms) in a single layer.

III. Characterizations

III.1. Structural, morphological and elemental characterizations

Powder X-ray diffraction (PXRD) patterns of the synthesized samples were recorded using a Rigaku Miniflex-600 (Japan) at scanning voltage of 40 kV and scanning current of 15 mA using monochromated Cu K_α radiation ($\lambda=1.5406 \text{ \AA}$). The phases were refined by means of Rietveld refinement as implemented in the FULLPROF program suite.

Surface morphology was characterized using a scanning electron microscope (NovaNanoSEM 450, USA) equipped with an X-ray energy-dispersive spectroscopy (EDS) system which was used for elemental analysis.

TEM and STEM imaging was performed at 300 kV accelerating voltage in an FEI Titan Themis 300 instrument, fitted with a X-FEG electron source, 3 lens condenser system and a S-Twin objective lens and SuperX- EDS system (for HAADF measurement). High-resolution TEM images were recorded with a resolution of 2048x2048 pixels with an FEI CETA-16M CMOS digital camera.

The MoB₂ sample was dissolved in a concentrated nitric acid solution and then analyzed by inductively coupled plasma optical emission spectrometry (ICP-OES) using a Perkin-Elmer Optima 7300DV ICP-OES with an SCD detector and an echelle optical system.

Nitrogen (N₂) adsorption–desorption isotherms data were obtained using an ASAP 2020, Micromeritics Inc., (USA) instrument at 77 K. The specific surface area of the synthesized

samples was estimated using the Brunauer–Emmett–Teller (BET) method in a relative pressure P/P_0 range from 0.05 to 0.30.

X-ray photoelectron spectroscopy (XPS) was performed on a Kratos AXIS Ultra DLD instrument equipped with an Al K_{α} monochromated X-ray source and a 165-mm mean radius electron energy hemispherical analyzer.

III.2. Electrode preparation and electrochemical measurements

Electrochemical measurements were conducted on an electrochemical workstation (Biologic VSP model, France) with a standard three-electrode system using a graphite rod as the counter electrode and saturated calomel electrode (SCE) as the reference electrode in an Ar saturated 0.5 M H_2SO_4 electrolyte at room temperature.

The working electrodes were prepared with 4 mg of synthesized samples, which were ultrasonically dispersed in 1 mL of isopropanol and deionized water mixture. Then 20 μ L of a 5% Nafion solution (Sigma Aldrich) was added to the above mixture and ultrasonicated for 30 min to form a homogeneous catalyst slurry. The catalyst slurry was coated over a carbon sheet (Sigracet) with area of 2×2 cm^2 . Finally, the catalyst-coated carbon sheet was dried at 70 °C for 120 minutes in hot air oven to remove the solvent from the electrode and to improve the bonding. The catalyst loading of the electrode was kept at ~ 0.5 mg/cm^2 for all the samples analyzed. The working electrodes were activated for several repeated cycles until the signals were stabilized.

The polarization curves were recorded from linear sweep voltammetry (LSV) measurements with sweep rate of 1 mV/s from 0 to -1.0 V. The cyclic stability was measured by cyclic voltammetry (CV) at a scan rate of 100 mV/s for 1000 cycles. The CV curves were also recorded with a graphite rod as counter electrode, to check if any dissolved Pt^{2+} (due to Pt corrosion in acids) has influenced the stability curve of the sample. All the potentials were referenced to a reversible hydrogen electrode (RHE) and iR-correction was applied.⁶

Finally, the electrochemically active surface area of the catalyst was estimated using double-layer capacitance (C_{dl}) from cyclic voltammograms at different scan rates (10 -100 mV/s) in the region of 0.1 – 0.2 V vs. RHE.

IV. Tables

Table S1: Fitting Parameters (peak position, full width at half maximum (FWHM) for Mo 3d and B 1s XPS spectra of molybdenum diboride and surface Mo- and B-oxides.

Sample	Species	Peak position for Mo 3d / B 1s (eV)	FWHM for Mo 3d / B 1s (eV)
Mo 3d			
MoB₂	Mo ⁰	228.5; 231.7	0.65; 1.01
Mo-oxides	Mo ³⁺	228.9; 232.5	1.93; 1.64
	Mo ⁴⁺	230.8	0.68
	Mo ⁶⁺	235.0	1.69
B 1s			
MoB₂	B ⁰	188.0; 188.6	1.92; 0.84
B₂O₃	B ³⁺	190.5; 191.8; 192.9	1.49; 0.74; 1.74

Table S2: Comparison of MoB₂ nanoparticles HER performance in acidic medium with other recent reports.

Samples	Particle size (*- from XRD)	Catalyst loading	Overpotential (mV/s) at 10 mV/s	Tafel slope (mV/dec)	Ref. No.
nano-MoB ₂	30-60 nm	0.5 mg	- 154	49	This work
bulk-MoB ₂	1-15 μm	0.2-0.3 mg	-250 (at 3.5 mV/s)	75	6
MoB	1-3 μm	2.5 mg	-215	55	7
Mo ₂ C	1-3 μm	1.4 mg	-210	56	7
MoP	19 nm*	71 μg	- 246	60	8
MoP	Bulk (very small particles)	0.86 mg	-145	54	9
Mo ₃ P	bulk	0.86 mg	-500	147	9
MoN/C	nanosheets	0.25 mg	-157	54.5	10
MoS ₂	monolayers	-	-170	60	11
MoS ₂	nanoparticles	0.28 mg	-	94	12
MoS ₂ /RGO	nanoparticles	0.28 mg	-160	41	12
MoS ₂ @GNR	nanosheets	0.05	-180	43.4	13
MoSe ₂	nanosheets	0.16 mg	-270	101	14
MoSe ₂ /RGO	nanosheets	0.16 mg	-150	69	14

Table S3: Calculated binding energy (ΔE_H) and Gibbs free energy (ΔG_H) of single H (25% H coverage) adsorption on Pt {111}, Mo {110}, Mo- and B-terminated MoB₂ {001} surfaces.

Binding site	Top (T)		Bridge (Bg)		Hollow (Ho)	
	ΔE_H (eV)	ΔG_H (eV)	ΔE_H (eV)	ΔG_H (eV)	ΔE_H (eV)	ΔG_H (eV)
Pt {111}	-0.41	-0.21	-0.32	-0.12	-0.33	-0.13
Mo {110}	+0.07	+0.27	-0.45	-0.25	-0.59	-0.39
Mo-terminated MoB ₂ {001}	-0.30	-0.10	-0.62	-0.42	-0.72	-0.52
B-terminated MoB ₂ {001}	-0.21	-0.01	-0.39	-0.19	+1.62	+1.82

Table S4: Calculated Gibbs free energy (ΔG_H) of H adsorption on different surfaces: the hollow (Ho) Pt {111}, Ho Mo {110}, Ho Mo-terminated MoB₂ {001} and bridge (Bg) B-terminated MoB₂ {001} at different H coverages. Bold values indicate the ΔG_H window enclosing $\Delta G_H = 0$.

H coverage	Gibbs free energy (ΔG_H) / eV			
	Pt {111}-Ho	Mo {110}-Ho	Mo-terminated MoB ₂ {001}-Ho	B-terminated MoB ₂ {001}-Bg
25%	-0.13	-0.39	-0.52	-0.19
50%	-0.07	-0.34	-0.39	-0.14
75%	-0.01	-0.44	-0.28	-0.06
100%	+0.08	-0.40	-0.21	+0.09

Table S5: Calculated binding energy (ΔE_H) and Gibbs free energy (ΔG_H) of single H (25% H coverage) adsorption on MoB_2 {110}, MoB_2 {101}, Mo- and B-terminated MoB_2 {100} surfaces.

Binding site	Top (T)		Bridge (Bg1)		Bridge (Bg2)		Hollow (Ho)	
	ΔE_H (eV)	ΔG_H (eV)						
MoB_2 {110}	+0.19	+0.39	+0.04	+0.24	+0.58	+0.78	-0.28	-0.08
Mo-terminated MoB_2 {100}	+0.03	+0.23	-0.09	+0.11	-0.33	-0.13	+0.32	+0.52
	Top (T1)		Top (T2)		Bridge (Bg1)		Bridge (Bg2)	
B-terminated MoB_2 {100}	-1.02	-0.82	+0.26	+0.46	-0.74	-0.54	+0.75	+0.95
	Top (T1)		Top (T2)		Top (T3)		Hollow (Ho)	
MoB_2 {101}	-0.02	+0.18	-0.19	+0.01	+0.08	+0.28	+0.07	+0.27

Table S6: Calculated Gibbs free energy (ΔG_H) of H adsorption on the hollow site (Ho) of MoB_2 {110}, on the bridge site (Bg2) of Mo-terminated MoB_2 {100} and on the top site (T2) of MoB_2 {101} surfaces at different H coverages. Bold values indicate the ΔG_H window enclosing $\Delta G_H = 0$.

H coverage	Gibbs free energy (ΔG_H) / eV		
	MoB_2 {110}-Ho	Mo-terminated MoB_2 {100}-Bg2	MoB_2 {101}-T2
25%	-0.08	-0.13	+0.01
50%	-0.07	-0.17	+0.05
75%	+0.10	-0.27	+0.54
100%	+0.11	-0.24	+0.82

V. Figures

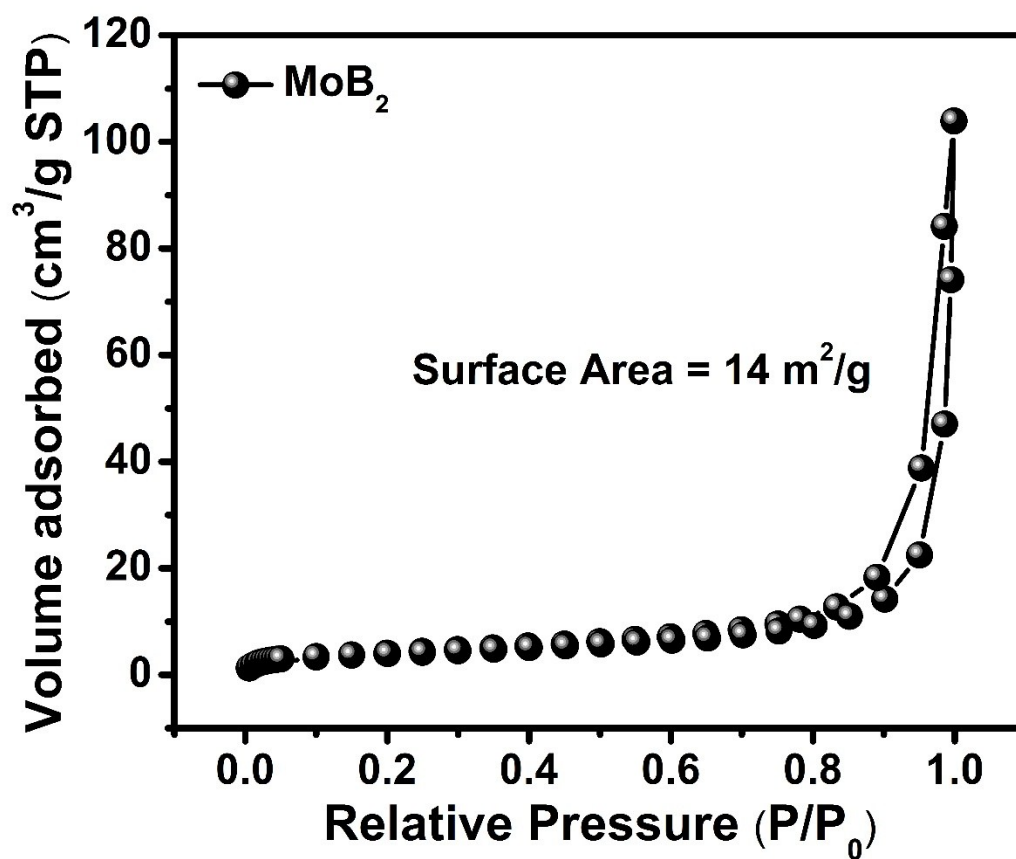


Figure S1. BET isotherm of MoB₂ from N₂ adsorption–desorption studies.

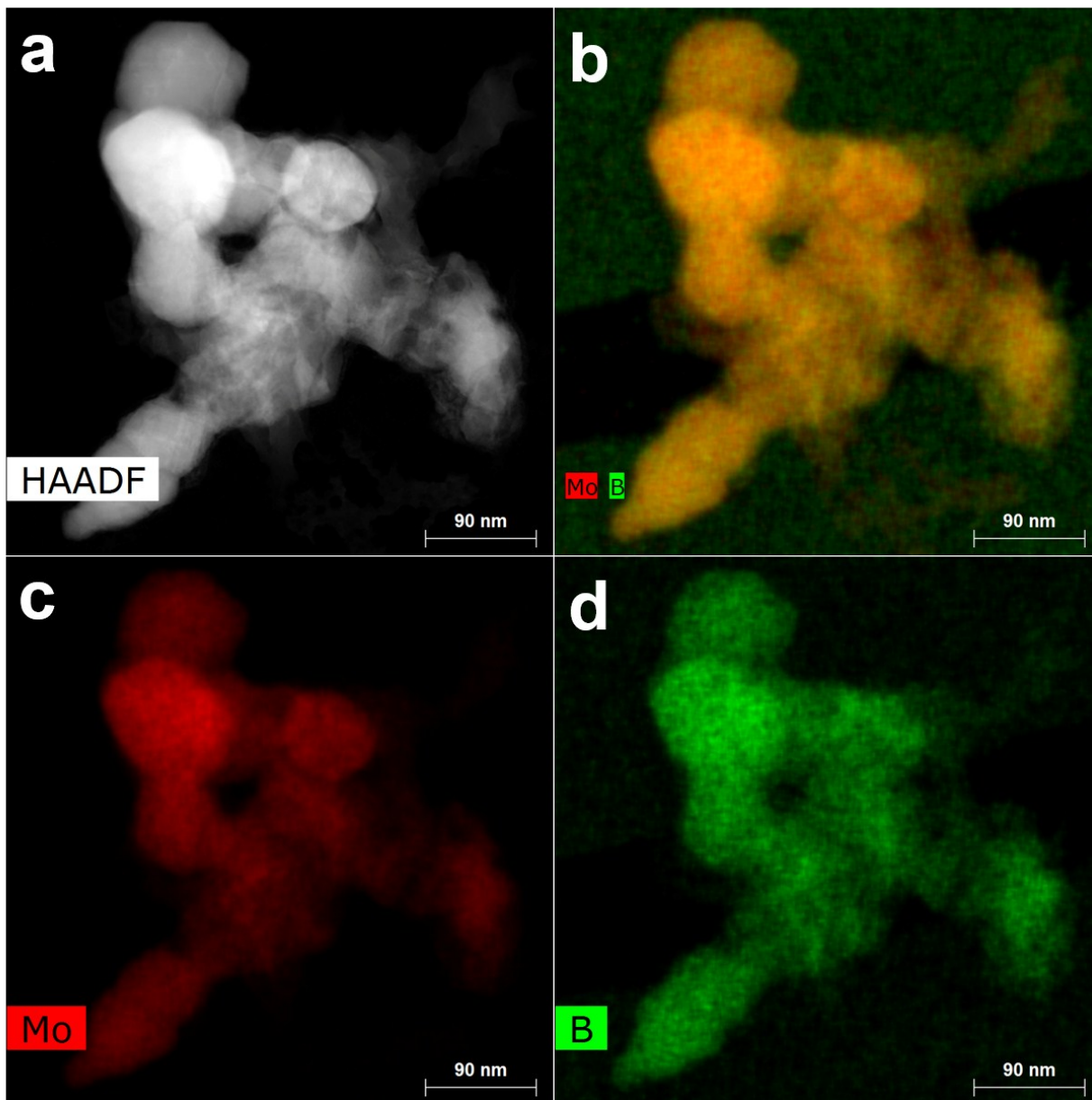


Figure S2. (a) HAADF-STEM (high-angle annular dark-field scanning transmission electron microscope) image of MoB₂ nanospheres, (b) corresponding EDS mapping, showing amorphous boron in the background (c) individual EDS map of Mo and (d) EDS map of B.

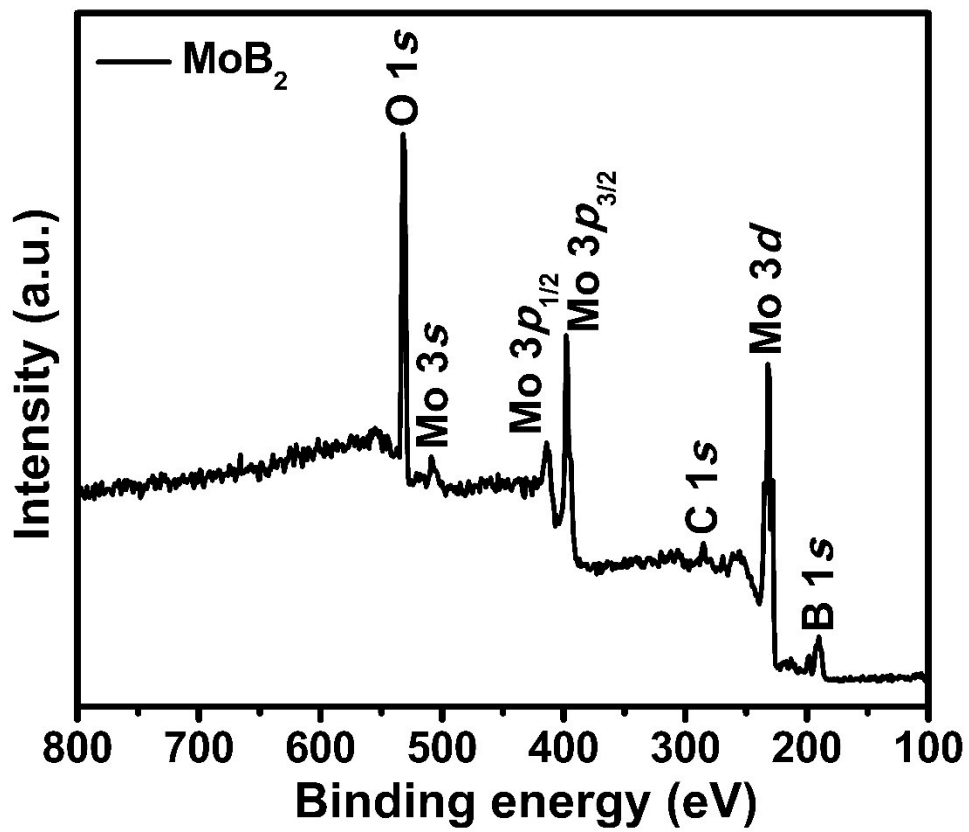


Figure S3. Full survey XPS spectrum of MoB₂.

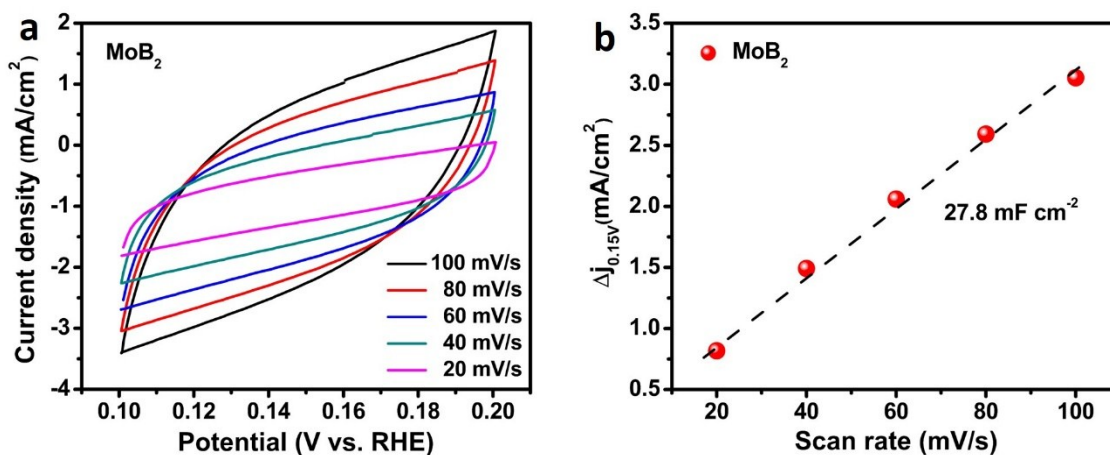


Figure S4. (a) C_{dl} measurements of MoB₂ from CV curves at different scan rates and (b) the measured capacitive currents plotted as a function of scan rate at 0.15 V vs. RHE.

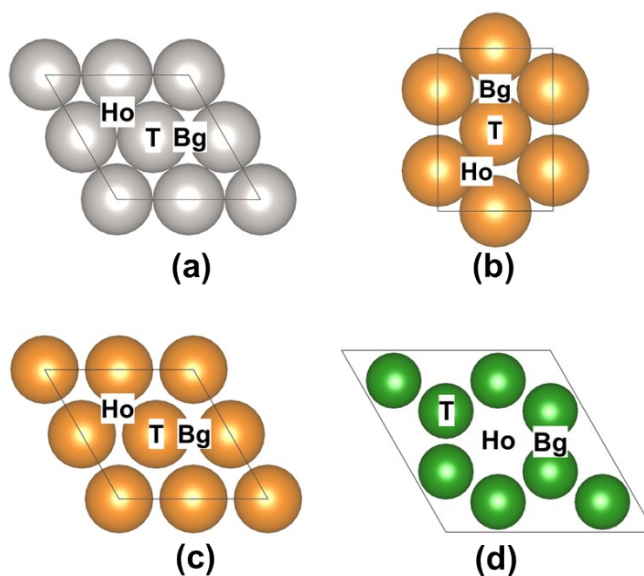


Figure S5. H adsorption site on (a) Pt {111}, (b) Mo {110}, (c) Mo-terminated MoB₂ {001} and (d) B-terminated MoB₂ {001} surfaces. T, Bg and Ho represents the top, the bridge and the hollow sites, respectively. Pt, Mo and B atoms are indicated by the grey, orange and green spheres, respectively.

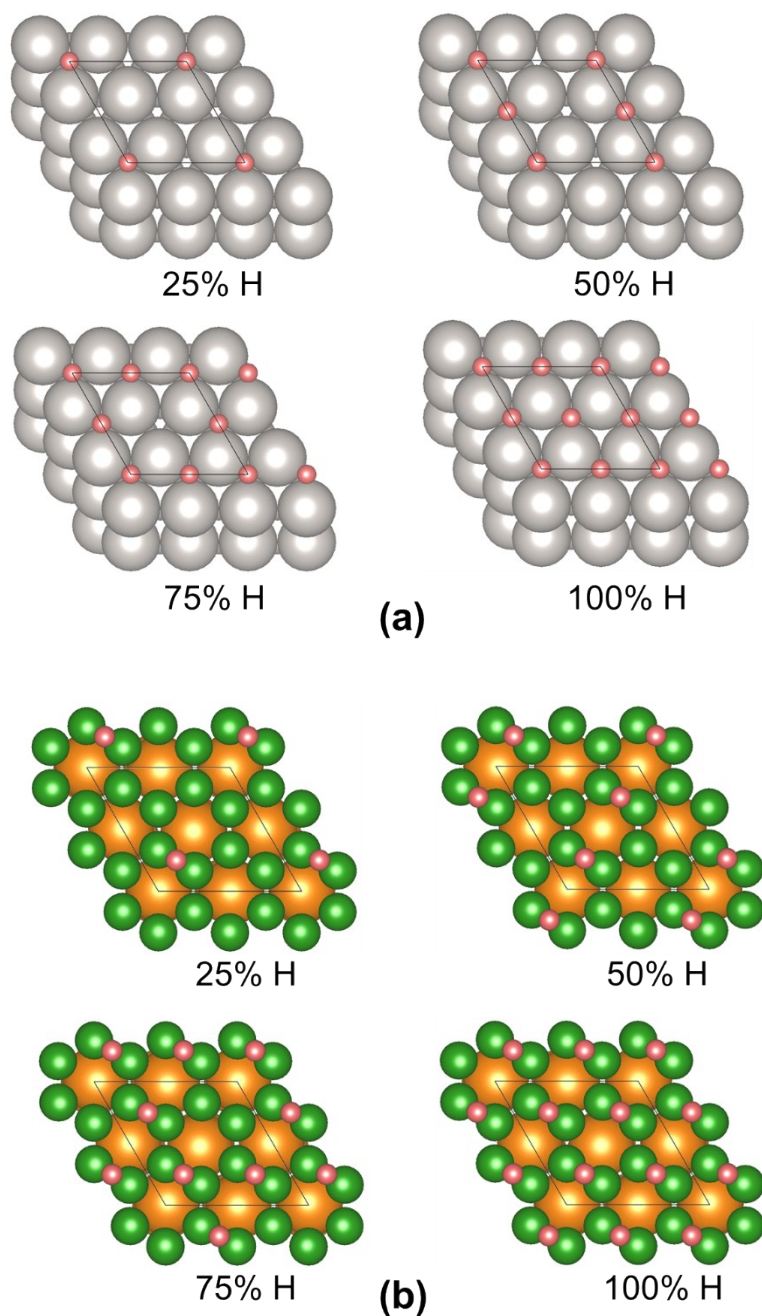


Figure S6. Top view of H adsorbed on (a) Pt {111} and (b) B-terminated MoB₂ {001} surfaces at different H coverages. The best H coverage configuration was chosen as to avoid short H contacts. Pt, Mo, B and H atoms are indicated by the grey, orange, green and light coral spheres, respectively.

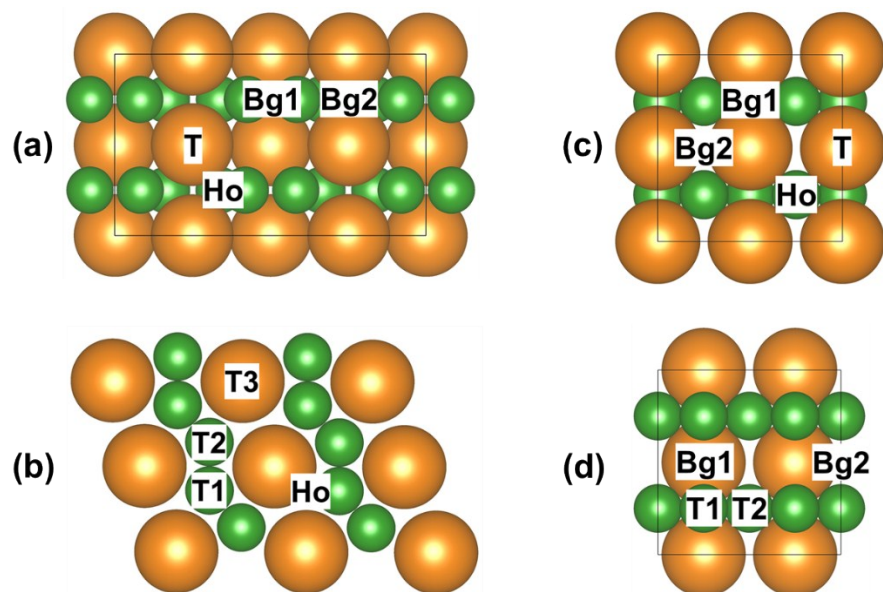


Figure S7. H adsorption site on (a) MoB_2 $\{110\}$, (b) MoB_2 $\{101\}$, (c) Mo-terminated MoB_2 $\{100\}$ and (d) B-terminated MoB_2 $\{100\}$ surfaces. T, Bg and Ho represents the top, the bridge and the hollow sites, respectively. Mo and B atoms are indicated by the orange and the green spheres, respectively.

VI. References

1. P. E. Blöchl, *Phys. Rev. B*, 1994, **50**, 17953-17979.
2. G. Kresse and D. Joubert, *Phys. Rev. B*, 1999, **59**, 1758-1775.
3. G. Kresse and J. Furthmüller, *Phys. Rev. B*, 1996, **54**, 11169-11186.
4. J. P. Perdew, K. Burke and M. Ernzerhof, *Phys. Rev. Lett.*, 1996, **77**, 3865-3868.
5. B. Hammer, L. B. Hansen and J. K. Nørskov, *Phys. Rev. B*, 1999, **59**, 7413-7421.
6. H. Park, A. Encinas, J. P. Scheifers, Y. Zhang and B. P. T. Fokwa, *Angew. Chem. Int. Ed.*, 2017, **56**, 5575-5578.
7. H. Vrubel and X. L. Hu, *Angew. Chem. Int. Ed.*, 2012, **51**, 12703-12706.
8. X. Chen, D. Wang, Z. Wang, P. Zhou, Z. Wu and F. Jiang, *Chem. Commun.*, 2014, **50**, 11683-11685.
9. P. Xiao, M. A. Sk, L. Thia, X. M. Ge, R. J. Lim, J. Y. Wang, K. H. Lim and X. Wang, *Energy Environ. Sci.*, 2014, **7**, 2624-2629.
10. W. F. Chen, K. Sasaki, C. Ma, A. I. Frenkel, N. Marinkovic, J. T. Muckerman, Y. Zhu and R. R. Adzic, *Angew. Chem. Int. Ed.*, 2012, **51**, 6131-6135.
11. H. Li, C. Tsai, A. L. Koh, L. Cai, A. W. Contryman, A. H. Fragapane, J. Zhao, H. S. Han, H. C. Manoharan and F. Abild-Pedersen, *Nat. Mater.*, 2016, **15**, 48-53.
12. Y. Li, H. Wang, L. Xie, Y. Liang, G. Hong and H. Dai, *J. Am. Chem. Soc.*, 2011, **133**, 7296-7299.
13. H. H. Gu, L. S. Zhang, Y. P. Huang, Y. F. Zhang, W. Fan and T. X. Liu, *RSC Adv.*, 2016, **6**, 13757-13765.
14. H. Tang, K. Dou, C.-C. Kaun, Q. Kuang and S. Yang, *J. Mater. Chem. A*, 2014, **2**, 360-364.